Title

The Second Extracellular Loop of the Adenosine A1 Receptor Mediates Activity of Allosteric Enhancers

Journal

Molecular Pharmacology, 85(2)

ISSN

0026-895X

Authors

Kennedy, Dylan P
McRobb, Fiona M
Leonhardt, Susan A
et al.

Publication Date

2014-02-01

DOI

10.1124/mol.113.088682

Peer reviewed

1521-0111/85/2/301–309$25.00
MOLECULAR PHARMACOLOGY

http://dx.doi.org/10.1124/mol.113.088682
Mol Pharmacol 85:301–309, February 2014

The Second Extracellular Loop of the Adenosine A_1 Receptor Mediates Activity of Allosteric Enhancers[S]

Dylan P. Kennedy, Fiona M. McRobb, Susan A. Leonhardt, Michael Purdy, Heidi Figler, Melissa A. Marshall, Mahendra Chordia, Robert Figler, Joel Linden, Ruben Abagyan, and Mark Yeager

Department of Pharmacology (D.P.K.), Department of Molecular Physiology and Biological Physics (S.A.L., M.P., H.F., M.C., R.F., M.Y.), Cardiovascular Research Center (M.A.M., R.F., M.Y.), Center for Membrane Biology (M.Y.), and Department of Medicine, Division of Cardiovascular Medicine (M.Y.), University of Virginia School of Medicine, Charlottesville, Virginia; the Skaggs School of Pharmacy and Pharmaceutical Sciences, University of California, San Diego, La Jolla, California (F.M.M., R.A.); and the La Jolla Institute for Allergy and Immunology (J.L.), La Jolla, California

Received July 22, 2013; accepted November 11, 2013

ABSTRACT

Allosteric enhancers of the adenosine A_1 receptor amplify signaling by orthosteric agonists. Allosteric enhancers are appealing drug candidates because their activity requires that the orthosteric site be occupied by an agonist, thereby conferring specificity to stressed or injured tissues that produce adenosine. To explore the mechanism of allosteric enhancer activity, we examined their action on several A_1 receptor constructs, including (1) species variants, (2) species chimeras, (3) alanine scanning mutants, and (4) site-specific mutants. These findings were combined with homology modeling of the A_1 receptor and in silico screening of an allosteric enhancer library. The binding modes of known docked allosteric enhancers correlated with the known structure-activity relationship, suggesting that these allosteric enhancers bind to a pocket formed by the second extracellular loop, flanked by residues S150 and M162. We propose a model in which this vestibule controls the entry and efflux of agonists from the orthosteric site and agonist binding elicits a conformational change that enables allosteric enhancer binding. This model provides a mechanism for the observations that allosteric enhancers slow the dissociation of orthosteric agonists but not antagonists.

Introduction

G protein–coupled receptors (GPCRs) are expressed throughout the body and regulate a broad range of physiologic actions through transmembrane signaling and coupling to heterotrimeric G proteins (Lin et al., 2013; Venkatakrishnan et al., 2013). As a result, GPCRs are the most targeted protein class in modern therapeutics (Overington et al., 2006). However, only a small fraction of known GPCRs have been targeted, leaving much room for new drug development through reverse pharmacology.

Allosteric modulators of GPCRs bind outside the conventional orthosteric ligand-binding site and elicit either a negative (negative allosteric modulators) or positive (positive allosteric modulators) effect on transmembrane signaling and receptor coupling. Adenosine receptors (ARs) are a family of GPCRs for the nucleoside adenosine, which consists of four members: A_1R, A_{2A}R, A_{2B}R, and A_3R. Positive allosteric modulators of the adenosine A_1 receptor (A_1R) are also known as allosteric enhancers (AEs). A number of AEs have been identified, targeted primarily to the A_1R subtype (Bruns and Fergus, 1990). Herein, we identify the A_1R AE binding site and suggest a mechanism by which these compounds act.

AEs decrease the dissociation kinetics of prebound orthosteric agonists and have no effect on the binding kinetics of orthosteric antagonists (Bruns and Fergus, 1990; Figler et al., 2003). A prerequisite for AE activity is occupancy of the orthosteric site by an agonist. This property makes AEs appealing as drug candidates because they act selectively in tissues actively releasing adenosine, such as a site of injury. For example, AEs of A_1Rs protect the heart (Mizumura et al., 1996), brain (Daval et al., 1989a,b), and kidney (Park et al., 2012) from ischemia reperfusion injury; inhibit lipolysis (Dhalla et al., 2009; Wojcik et al., 2010); and decrease neuropathic pain (Li

This work was supported by the National Institutes of Health National Institute of General Medical Sciences and the National Institutes of Health National Heart, Lung, and Blood Institute [Grants R01-HL048908, R01-HL056111, R01-GM071872, U01-GM094612, and U54-GM094618].
D.P.K. and F.M.M. contributed equally to this work.
dx.doi.org/10.1124/mol.113.088682.
[S] This article has supplemental material available at molpharm.aspetjournals.org.

ABBREVIATIONS: 1-277, 6-(3,4-methylenedioxyphenyl)-8*H*-indeno[1,2-*d*]thiazol- 2-ylamine hydroiodide; 4-41, bis-(2,2′-*N*,*N*-piperdinecarboxyamidephenyl)-disulfide; A_1R, adenosine A_1 receptor; AE, allosteric enhancer; ALiBERO, automated ligand-guided backbone ensemble receptor optimization; AR, adenosine receptor; ATL525, 2-amino-4,5,6,7-tetrahydro-benzo[*b*]thiophen-3-yl)biphenyl-4-yl-methanone; ECL, extracellular loop; GPCR, G protein–coupled receptor; GTPγS, guanosine 5-(γ-thio)triphosphate; hA_1R, human adenosine A_1 receptor; HEK293, human embryonic kidney cell line; ^{125}I-ABA, ^{125}I-N^6-(3-iodo-4-aminobenzyl)adenosine; NECA, adenosine-5′-*N*-ethylcarboxamide; NSQ AUC, normalized square-root area under curve; PD 81,723, (2-amino-4,5-dimethyl-3-thienyl)-[3-(trifluromethyl)-phenyl]-methanone; PDB, Protein Data Bank; SAR, structure–activity relationship; TM, transmembrane; VLS, virtual ligand screening; XAC, xanthine amine congener.

et al., 2002, 2003). An additional advantage of AEs is that their selectivity for tissues that generate adenosine may obviate the limitation of A_1R orthosteric agonists, which produce heart block as a dose-limiting side effect.

Identification of the molecular determinants of AE activity has the potential to advance mechanistic studies and clinical development. Mathematical modeling is one approach that has been used to gain mechanistic insight into allosteric enhancers (May et al., 2007; Canals et al., 2011, 2012; Heitman et al., 2012). In general, the models involve simplified systems, including the receptor, the orthosteric ligand, and the allosteric enhancer. Such modeling predicted that the A_1R allosteric site resides along the path followed by a ligand to reach the orthosteric site (Pietra et al., 2010). Although unable to identify specific residues or protein domains, the mathematical models provide guidance for the design of experiments. Nevertheless, despite 23 years of research since the initial discovery of A_1R AEs (Bruns and Fergus, 1990), a detailed understanding of their mechanism of action remains largely unknown.

Drug development of AEs has also been impeded in part by difficulties in studying their physiologic actions in vivo. In previous studies, AE activity was reported to vary in vitro and in vivo among species such as human, mouse, guinea pig (Amoah-Apraku et al., 1993; Kollias-Baker et al., 1994), dog (Mizumura et al., 1996), and rat (Bruns and Fergus, 1990). However, many of these investigations used assays that do not distinguish AE activity from competitive antagonist activity, which is also possessed by AE compounds to a variable extent. Consequently, the measured activities were a composite of allosteric and competitive antagonist effects. To obviate this issue, kinetic methods are considered the most sensitive and direct measurement of allosteric modulation of GPCRs (Christopoulos and Kenakin, 2002).

An additional impediment to the drug development of AEs is that their binding sites have not been precisely determined. GPCRs possess seven transmembrane domains, three intracellular and three extracellular loops, an extracellular N terminus, and an intracellular C terminus. Residues in each of these domains affect allosteric modulation (Conn et al., 2009; Göblyös and IJzerman, 2011). In the muscarinic receptors, allosteric sites have been identified in the second extracellular loop (ECL) 2 (Voigtländer et al., 2003) and near transmembrane domain (TM) 6 and ECL3 (Ellis et al., 1993). However, allosteric sites are not necessarily conserved between GPCR subfamilies so that allosteric targeting of each receptor is an individual pursuit (Christopoulos and Kenakin, 2002; Birdsall and Lazareno, 2005).

For adenosine receptors, a study using orthosteric agonists tethered to AEs (so-called bitopic ligands) suggested that the ECL2 of A_1R may be an AE binding region (Narlawar et al., 2010). In addition, a recent study showed that mutation of ECL2 residues W156 and E164 in A_1R-modified AE activity (Peeters et al., 2012). Our studies sought to define the AE binding site of A_1R in more detail.

Materials and Methods

Radioligand Binding. Radioligand binding was performed as previously described (Tranberg et al., 2002; Figler et al., 2003). We used an AE activity assay that measures ligand dissociation and therefore is not complicated by AE antagonist activity, as the receptor is prebound to orthosteric ligand. Receptors (10 μg in 50 μl) and the A_1R-specific agonist ^{125}I-ABA [0.5 nM in 50 μl; ^{125}I-N^6-(3-iodo-4-aminobenzyl)adenosine] are brought to equilibrium binding by a 120-minute incubation at ambient temperature. At this concentration, ^{125}I-ABA specifically binds to A_1R (Supplemental Fig. 1). In the kinetic assay that we used (Figler et al., 2003), we observed that the effects of allosteric enhancer were directly related to the time of incubation. For each assay, the AE was added for a consistent period (10 minutes). Ten minutes was selected because it was sufficient for the AE to bind to A_1R but sufficiently short that any effects on the equilibrium binding of the prebound, orthosteric agonist radioligand were minimized.

Finally, 50 μl containing 50 μM guanosine 5-(γ-thio)triphosphate (GTPγS) and 100 μM xanthine amine congener (XAC) are added for 15 minutes, which is sufficient to evaluate the AE-induced stability to GTPγS-induced dissociation. XAC is a nonspecific AR antagonist that is added to ensure that ^{125}I-ABA does not reassociate with the receptor. The residual binding is adjusted to a 100-point scale, giving a unitless value for the enhancer activity. An enhancer score of 0 is fully decoupled (GTPγS and XAC with no added AE), and a score of 100 is equilibrium binding (no added AE, GTPγS, or XAC). The AE score was measured at the end of the 10-minute incubation period, in which case the score ranged from 0 to 100.

Statistical Analysis. AE activity measurements were conducted in triplicate on cell lysates from the species variants or receptor mutants. Each lysate was derived from at least two parallel-derived stable cell lines or at least three independent transient transfections. Results were compared by two-way analysis of variance at each concentration point and fitted for EC_{50} and maximal AE activity (regression line asymptote) in Prism 5.0 (GraphPad Software, Inc., La Jolla, CA). Direct comparisons (log EC_{50} or maximum AE activity) were made using the Student's t test, in which three to five experiments were averaged. Curves were also compared by the extra sum-of-squares F test in Prism 5.0. Error was presented as ± S.E.M.

A_1R Mutagenesis. Human and dog A_1R cDNAs were subcloned into the pDoubleTrouble vector (hexahistidine and FLAG peptide-tagged CLDN10B vector) (Robeva et al., 1996) for stable expression in mammalian cells. Mutagenesis was performed using QuikChange Lightning and/or QuikChange Multi Lightning (Agilent Technologies, Santa Clara, CA). Primers were synthesized per Agilent guidelines. All mutations were confirmed by sequencing (GENEWIZ, South Plainfield, NJ). The A_1R affinity for ^{125}I-ABA was not affected significantly by the reported mutations.

4× Alanine Scan of ECLs. The mutations introduced into the A_1R-pcDNA3.1+ background were NIGP 70 AAAA; QTY 74 AAA; FTH 77 AAA; NNLS 147 AAAA; AVER 151 LAAA; AVER 151 QAAA; AWAA 155 LALL; AWAA 155 GANH; NGSM 159 AAAA; GEP 163 AAA; VIK 166 AAA; PS 261-2 AA, HK 264-5 AA; C260A and C263A (Supplemental Table 1). Receptor mutants were transiently transfected into human embryonic kidney (HEK293) cells using LipofectAMINE 2000 (Invitrogen, Carlsbad, CA) per the manufacturer's instructions. To allow sufficient time for protein expression, cells were lysed and prepared for binding 72 hours post transfection.

Generation of Stable Cell Lines. Plasmids were purified with NucleoBond Xtra Midi kit (Macherey-Nagel GmbH, Düren, Germany), and receptor mutants were transfected stably into HEK293 cells using LipofectAMINE 2000. Cells were selected for plasmid expression with G418 (1 mg/ml; Inalco Pharmaceuticals, San Luis Obispo, CA), screened for A_1R expression by agonist (^{125}I-ABA) radioligand binding ± adenosine-5′-*N*-ethylcarboxamide (NECA) as a measure of nonspecific binding. HEK293 cells were cultured with 10% CO_2 at 37°C in Dulbecco's modified Eagle's medium (Invitrogen) containing 10% fetal bovine serum (Gemini Bio-Products, West Sacramento, CA) and 1% antibiotic/antimycotic (Invitrogen). Cell lysates were prepared by repeated (10–12) passes through a 28.5-gauge needle (BD Biosciences, San Jose, CA) at 4°C in a hypotonic solution (10 mM HEPES, pH 7.4) containing 2 U/ml of adenosine deaminase (Roche Applied Science, Indianapolis, IN,) (Robeva et al., 1996; Figler et al., 2003). Radioligand binding was conducted as previously reported with identical reagents

and materials (Figler et al., 2003). Several A_1R mutants were created in cell lines to delineate specific residues responsible for differences between human and dog A_1R (Supplemental Table 2). Single alanine mutants created to identify specific residues involved in binding were N147A, N148A, L149A, and S150A (Supplemental Table 3). K_D and B_{max} data were determined for each mutation or cell line (Supplemental Table 4).

Allosteric Enhancers. Synthesis and characterization of AE 1-227 [6-(3,4-methylenedioxyphenyl)-8*H*-indeno[1,2-*d*]thiazol-2-ylamine hydroiodide] have been reported previously (compound 3ab) (Chordia et al., 2005). AEs ATL525 (2-amino-4,5,6,7-tetrahydro-benzo[*b*]thiophen-3-yl) biphenyl-4-yl-methanone) (Tranberg et al., 2002) and 1-277 were evaluated at concentrations <100 μM. Concentrations >100 μM require dimethylsulfoxide levels known to disrupt the radioligand binding assay. It is difficult to determine whether AEs have direct agonist effects because cells and membranes are frequently contaminated with low levels of adenosine. It is clear AEs produce much stronger effects in the presence of orthosteric agonists than in their absence. ATL525 displays minimal antagonist effects, as previously demonstrated (Figler et al., 2003).

Molecular Modeling. Ligand preparation, sequence alignment, homology modeling, docking, and analyses were carried out in ICM version 3.7-3a (Molsoft L.L.C., La Jolla, CA) (Abagyan and Totrov, 1994; Cardozo et al., 1995). A multiple-sequence alignment was generated between human (h) A_1R, $A_{2A}R$, $A_{2B}R$, A_3R and A_1R for the species of interest (dog, mouse, rat, chicken, and rhesus monkey; (Supplemental Fig. 2). Building of the initial homology model of hA_1R was based on the high-resolution, agonist-bound, crystal structure of the adenosine $A_{2A}R$ receptor [Protein Data Bank (PDB) ID 3QAK] (Xu et al., 2011) after removal of the T4-lysozyme insertion. The backbone conformations of the well-aligned regions were inherited from the template, whereas the insertions and deletions were modeled by exhaustively searching a library of PDB fragments for loops of similar length and termini orientation. The loop searches were performed for the following regions in hA_1R: A155–G163 (P149–H155 in $hA_{2A}R$), which were disordered in the template, and L211–Q223 (L208– R222 in $hA_{2A}R$), which was replaced by the T4-lysozyme in the template. The loop fragments were sampled and minimized in the context of the model to find an optimal conformation for each loop. The model was then subjected to extensive side-chain sampling and refinement.

Potential ligand binding sites in the initial hA_1R homology model were predicted using the ICM PocketFinder algorithm (An et al., 2005). Residues that were identified as surrounding the potential AE binding site in ECL2 were used to define the binding site for docking (F77, N148, E153, A157, M162, G163, V166, I167, K173). The model was subjected to refinement and evaluation using the Automated Ligand-guided ALiBERO algorithm (Rueda et al., 2012). This algorithm searches the conformational space of the proposed binding site in the initial hA_1R homology model by Elastic Network Normal Mode Analysis of the neighboring backbone and side chain atoms. ALiBERO evaluates multiple generated conformations for their compatibility with the activity of known AEs. For this evaluation, we used a set of 58 compounds (Supplemental Table 5) that were previously characterized for A_1R allosteric modulator activity: 33 "active" compounds (Göblyös and IJzerman, 2011) and 25 "inactive" compounds (Bruns et al., 1990). (Inactive compounds were defined as chemicals with A_1R enhancement of less than 10%.) The library of known active and inactive compounds was screened against 100 ALiBERO-generated receptor conformations using the ICM ligand docking and scoring module (Supplemental Fig. 3), and a receiver-operating characteristic curve was built for each receptor conformation. The normalized square-root area under curve (NSQ_AUC) (Katritch et al., 2011, 2012) was also calculated. The ability of the receptor conformations to discriminate active compounds from inactive compounds in virtual ligand screening (higher NSQ_AUC) correlates with increased reliability of the model. Using ALiBERO, the five receptor conformations that contributed to the ensemble with the highest NSQ_AUC were resubjected to the Elastic Network Normal Mode Analysis sampling procedure, and this was repeated four times to further optimize the hA_1R homology models. The receptor conformations from the final ensemble with the highest NSQ_AUC were visually inspected, and the docked binding modes of the AEs were compared with the structure–activity relationship (SAR) of known AEs. Based on visual inspection of the receptor-ligand complexes, the model of hA_1R in complex with a 2-aminothiophene AE that satisfied the known SAR was retained for further docking studies.

To evaluate the species differences for A_1R, ECL2 in the hA_1R homology model was mutated to ECL2 for each species of interest (dog, mouse, rat, chicken, and rhesus monkey). The complexes underwent minimization where the 2-aminothiophene was tethered to its initial position (tzWeight = 0.1), "soft" van der Waals terms were used (vwMethod = 2), and side-chains within 8 Å were minimized for up to 10,000 iterations, mimicking the induced fit effect of ligand binding. The AEs PD 81,723 [(2-amino-4,5-dimethyl-3-thienyl)-[3-(trifluromethyl)-phenyl]-methanone] and ATL525 were computationally docked into the proposed allosteric site in ECL2 of all species, and their interactions with the receptor were assessed.

Results

Overall Strategy. To comprehensively explore the AE binding site in A_1R, we examined the activity of AEs on (1) species variants, (2) species chimeras, (3) alanine scanning mutants, and (4) targeted site-specific mutants. To yield more accurate measurements of AE activity, we used a kinetic assay that is not influenced by competitive antagonism (Tranberg et al., 2002; Figler et al., 2003). In addition, our test compound, ATL525, is a highly efficacious AE with limited antagonist activity.

To quantify AE activity, we used a system that "scores" AE activity, with results ranging from 0 to 100, where 0 represents no effect of the AE on orthosteric agonist dissociation kinetics and 100 represents equilibrium binding, or no orthosteric agonist dissociation. Reported pharmacological parameters were calculated from curves fit to the raw scores. GTPγS-insensitive binding, such as that scored in this assay, is a unique reporter for AE activity that is minimally affected by ^{125}I-ABA binding affinity. AE affinity, cooperativity with agonist, and changes in receptor–G protein coupling are all inter-related in every assay system.

Agonist dissociation experiments using ATL525 allowed us to evaluate the effects of AEs directly on the receptor, not the whole cell, which results in a more precise evaluation of AE binding. Because of the effects of competitive antagonism, measurement of dissociation kinetics gives the most pure assessment of AE activity. We also determined the EC_{50} of AEs as a measure of AE binding affinity. The EC_{50} is reported as an index of AE affinity, which has never been experimentally reported. All reported mutations were evaluated for changes in GTP sensitivity, and none was observed.

The structural interpretation of our mutagenesis and activity experiments was guided by an A_1R homology model based on the X-ray crystal structure of the agonist-bound $hA_{2A}R$ (PDB ID 3QAK) (Xu et al., 2011). Further computational analysis used the ICM PocketFinder algorithm (An et al., 2005), and the identified allosteric binding pocket was refined using the ALiBERO protocol (Katritch et al., 2010, 2012; Rueda et al., 2012). Taken together, these analyses defined an AE binding pocket in ECL2, and we propose that AEs function by

occupying this vestibule and blocking agonist dissociation from the high affinity (R*) state of the receptor.

AE Activity Does Not Correlate with Overall Sequence Identity between Species. We first compared A_1R sequence variability between a number of species with the relative activities of the potent AE, ATL525, which lacks antagonist activity (Fig. 1, inset) (Figler et al., 2003). Experiments on the dissociation kinetics of orthosteric agonist revealed a range of AE activities among these species (Fig. 1). Agonist dissociation from the rhesus monkey A_1R is the slowest, followed by human and chicken, with dog, rat, and mouse being the least affected by ATL525. The A_1R sequence variability, relative to monkey, are human, 0.3% (1 residue of 327); mouse and rat, 4.9% (16/327); dog, 6.1% (20/327); and chicken, 19.4% (63/325). The order of AE activities does not correlate with overall sequence variability. This finding suggests that AE activity is governed by specific amino acids in discrete binding or signaling domains.

Chimeric Mutagenesis Indicates That Residues 150 and 162 Mediate AE Activity. Since AE activity varies among species, we created species chimeras to identify residues responsible for AE activity differences. Analysis of the sequence alignments between species revealed that the ECL2 (residues 147–175) and the C terminus (residues 291+) regions of the protein contain the highest sequence variability (Fig. 2A). On the basis of previous studies of receptor species chimeras, the C terminus and third intracellular loop are not involved in AE activity (Bhattacharya et al., 2006). However, as noted already, there is evidence that AEs bind to ECL2 (Narlawar et al., 2010); hence, we focused our attention on this region.

Excluding the chicken A_1R, only ECL2 residues 147–162 are variable among species, and we created a set of chimeras between the human and dog receptors spanning this region (Supplemental Table 1). Our experiments identified two human-to-dog mutations that reduced the activity of AEs on hA_1Rs to that of dog A_1R: S150G and M162G (Fig. 3B). Compared with hA_1R, activity on the dog A_1R is decreased by 17.7 ± 1.3 enhancer score points. AE score on the hA_1R-dECL2 chimera decreases by 29.6 ± 0.34 ($P < 0.0001$), S150G decreases by 27.9 ± 0.88 ($P < 0.001$), and M162G decreases by 16.9 ± 2.2 ($P < 0.01$) enhancer score points.

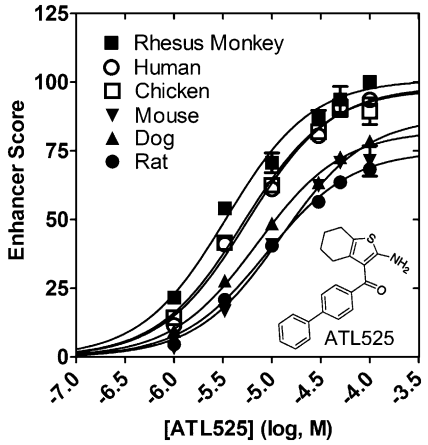

Fig. 1. Variation in interspecies AE activity. Enhancer activity score (0–100) among species is plotted against concentration of ATL525; (■) rhesus monkey, (○) human, (□) chicken, (▼) mouse, (▲) dog, (●) rat. Each point is the mean ± S.E.M. (Inset) Chemical structure of ATL525.

The species differences in AE activity are not due solely to these two residues, since introducing the reciprocal mutations in dog A_1R did not restore activity. To further investigate this result, we built a homology model of hA_1R based on the crystal structure of agonist-bound $hA_{2A}R$ (PDB ID 3QAK) (Xu et al., 2011). In the hA_1R homology model, residues 150 and 162 reside at opposite sides of ECL2, potentially defining the boundary of a binding site (Fig. 3A).

Alanine Scanning of ECL2 Confirms That Residues 150 and 162 Mediate AE Activity. To further define the role of ECL2 in AE activity, we conducted an alanine scan, in which blocks of four consecutive residues from all three hA_1R ECLs were mutated to alanine (Fig. 2B; Supplemental Table 2). In particular, these experiments were designed to identify conserved residues between dog and human A_1R that alter AE activity. Two of the mutants caused large decreases in AE activity: NNLS 147 AAAA and NGSM 159 AAAA. Our initial experiments used transient transfections, and we also generated stable cell lines of these two mutants, as well as mutants in which residues 147–150 (NNLS) were individually mutated to alanine. AE activity measurements revealed that only the S150A mutation significantly decreased AE activity compared with human, with AE sensitivity similar to NNLS 147 AAAA (Fig. 3C). The involvement of ECL2 residue M162 was also confirmed by alanine scanning. The NGSM 159 AAAA mutation reduced AE activity to a similar extent as the M162G species chimera mutant. The efficacy of AEs is significantly reduced by these mutations compared with native hA_1R. Maximum AE activity decreased for NNLS 147 AAAA by 37.3 ± 6.3 ($P < 0.0001$) and for S150A by 28.4 ± 2.6 ($P < 0.001$). Compared with hA_1R, the S150A mutation shifts the EC_{50} from 2.9 μM ± 0.19 to 5.5 μM ± 0.36 ($P < 0.05$), suggesting that this mutation affects the ability of the AE to occlude the orthosteric binding pocket more than to affect AE binding affinity. A recent alanine scanning study (Peeters et al., 2012) used an indirect yeast growth reporter assay that is susceptible to antagonist activity of AEs, effects of agonist-AE cooperativity, and signal amplification (discussed in Stewart et al., 2009). Nevertheless, these experiments showed that the mutations W156A and E164A in ECL2 decreased the effects of the AE PD 81,723. Agonist dissociation measurements with receptor chimeras and alanine mutants demonstrated that mutation of hA_1R residue S150 to either G or A significantly decreases the activity of ATL525 (Fig. 3B). The decrease in AE activity was not additive with M162G, suggesting that S150 and M162 both participate in AE binding.

Identification of ECL2 residues S150 and M162 as mediators of AE activity can potentially explain the A_1R subtype specificity of 2-aminothiophene AEs. The A_1R and the AE-insensitive $A_{2A}R$ differ in 19 of 34 residues in ECL2. In addition, the A_1R has only one disulfide bond in ECL2, whereas the $A_{2A}R$ contains three. As a result, the $A_{2A}R$ ECL2 is likely to have reduced conformational flexibility compared with ECL2 in the A_1R, and this constraint may impede AE binding compared with the A_1R.

ECL2 Mutagenesis Affects the Activities of Two Chemical Classes of AEs. The first described A_1R AEs were 2-aminothiophenes, exemplified by PD 81,723. Thereafter, more efficacious compounds were developed such as ATL525 (van der Klein et al., 1999; Baraldi et al., 2000; Tranberg et al., 2002). We recently demonstrated that a second class of AEs, 2-aminothiazole compounds, also possess AE

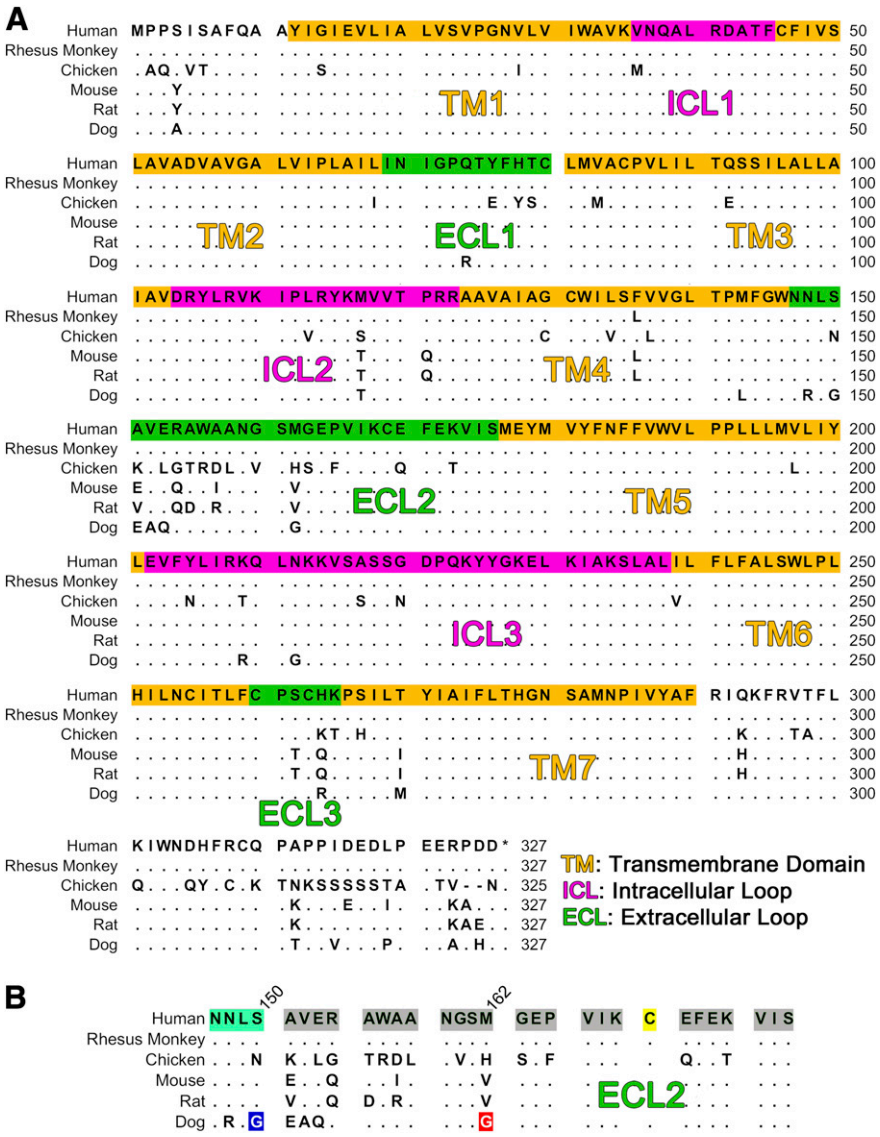

Fig. 2. (A) hA_1R amino acid sequence alignment of the species analyzed for AE activity. Dots (·) indicate conserved residues. Dashes (-) indicate gaps. ECL, green; ICL, intracellular loops, magenta; TM, yellow. Residue numbers are indicated at the end of each row for each species. (B) Summary of ECL2 mutations. Blocks of three and four amino acids denote groups of residues mutated in alanine scans. Positions 150 (blue) and 162 (red) were identified by swapping residues between species.

activity (Chordia et al., 2005). We evaluated the AE activity of the 2-aminothiazole compound 1-277 (Fig. 3D, inset) on native hA_1R and the S150A and M162G mutants. Although the M162G mutation had no effect on the AE score of 1-277, the S150A mutation decreased the 1-277 AE score, similar to ATL525 (Fig. 3). Since AEs from both chemical classes display reduced activity on receptors bearing the mutation S150A, this residue may interact with the common feature between these structurally different chemical classes: a 2-amino-substituted, sulfur-containing, five-membered ring. The general inference is that these two classes of AEs likely share a common A_1R binding site.

Molecular Modeling, In Silico Screening, and Docking Simulations Identify an AE Binding Pocket in ECL2. On the basis of the involvement of S150 and M162 in AE activity, we sought to further investigate the structural details of AE binding using molecular modeling, in silico screening, and docking simulations. A potential pocket that included residues S150 and M162 in ECL2 was identified in our hA_1R homology model using the ICM PocketFinder algorithm (Fig. 4, A and D, red surface) (An et al., 2005). The proposed ECL2 binding site is a solvent-exposed cleft that is accessible to AEs. Notably, similar pockets formed by ECL2 were present in homology models of A_1Rs from several other species (Supplemental Fig. 4).

Comparison of the agonist-bound crystal structure of $A_{2A}R$ with the inactive, antagonist-bound structure reveals a distinctive coupled movement between the antiparallel β-sheets in ECL1 and ECL2 and TM3. In the antagonist-bound structure of $A_{2A}R$ (PDB ID 4EIY) (Liu et al., 2012), TM3 contains a kink (Fig. 5, blue); however, in the agonist bound structure (PDB ID 2YDV (Lebon et al., 2011) TM3 is straightened in an outward, piston-like movement of ~2.5 Å (Fig. 5, orange), breaking contacts with TM5 and TM6. At the same time, agonist binding results in a repositioning of the β-sheets adjacent to TM3 in ECL1 and ECL2 (Fig. 5, black arrow). It should be noted that the coupled movement of the antiparallel β-sheets and TM3 was observed in both the thermostabilized (Lebon et al., 2011) and the fused T4 lysozyme (Xu et al., 2011) agonist-bound $A_{2A}R$ structures. This mechanism may also be involved in the

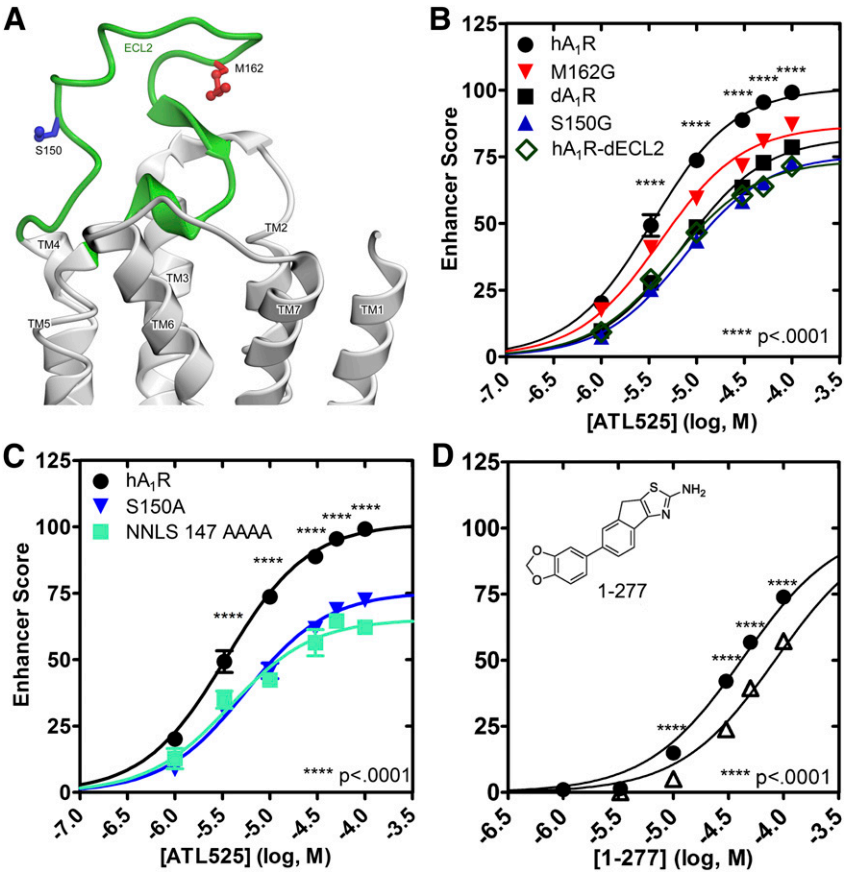

Fig. 3. Mutation of residues S150 or M162 decreases AE activity. (A) hA_1R homology model based on $hA_{2A}R$ structure (PDB ID 3QAK): backbone (gray), ECL2 (green), S150 (blue), and M162 (red). (B) ATL525 AE scores (0-100). (●) hA_1R, (▼, red) hA_1R M162G, (■) dA_1R, (▲, blue) hA_1R S150G, (◇) hA_1R-dECL2 (hA_1R background with dog A_1R [dA_1R] ECL2 residues). ****$P < 0.0001$. (C) Activity of hA_1R S150A and hA_1R NNLS 147 AAAA compared with hA_1R. (●) hA_1R, (▼, blue) hA_1R S150A, (■, cyan) hA_1R NNLS 147 AAAA. ****$P < 0.0001$. Data plotted ± S.E.M. (D) AE dose-response curves for the 2-aminothiazole, 1-277. (●) hA_1R, (△), hA_1R S150A. ****$P < 0.0001$. Each point is the mean ± S.E.M. (Inset) Structure of 1-277.

activation mechanism of A_1R. Thus, AE binding to the proposed allosteric site in ECL2 (Fig. 5b, red surface) may affect the conformational equilibrium of TM3 in hA_1R and bias the receptor toward the active state. Although further insights into this coupled mechanism for hA_1R will require crystal structures of the active and inactive states of hA_1R, we speculate that a conformational switch in the receptor on orthosteric agonist binding accounts for the differential effects on association and dissociation kinetics.

To improve our model of the AE binding site, the hA_1R homology model was refined using the ALiBERO protocol (Rueda et al., 2012). ALiBERO uses elastic-network normal mode analysis to generate multiple binding site conformations and virtual ligand screening to identify models that best discriminate between "active" and "inactive" compounds. For this analysis, a library of known A_1R AEs ("actives") (Göblyös and IJzerman, 2011), as well as compounds that had little or no AE activity ("inactives") (Bruns et al., 1990), was used (Supplemental Table 3). The ability to distinguish active from inactive compounds in virtual ligand screening is correlated with increased accuracy in predicting atomic contacts within ligand binding sites (Katritch et al., 2010; Kufareva et al., 2011; Rueda et al., 2012). Consistent with the crude character of the initial hA_1R homology model, the putative ECL2 pocket did not recognize the known AEs, where the NSQ_AUC of only 1.8 is close to a random NSQ_AUC value of 0. After model optimization using ALiBERO, the best receptor conformation ensemble recognized the known AEs with an NSQ_AUC of 89.8 (approaching the ideal of 100), indicating that the refined models could better predict atomic contacts between A_1R and AEs.

Docking PD 81,723 and ATL525 into the optimized receptor conformations illustrated how AEs could bind to the proposed allosteric site formed by ECL2 (Fig. 4, B–F; Supplemental Figs. 5 and 6). Superposition of the docked poses of ATL525 and PD 81,723 revealed a similar binding mode for the two AEs, including the presence of a hydrogen bond between the 2-amino group and S150, a residue independently implicated in AE binding in mutagenesis experiments (Fig. 3, B and C). The 4- and 5-positions of the thiophene are solvent exposed and the 3-benzoyl group is directed toward the back of the site formed by ECL2. Docking calculations with PD 81,723 demonstrated a similar binding mode.

The increased length of ATL525 versus PD 81,723 (~12 Å and ~9 Å, respectively) may account for its greater AE activity. Specifically, ATL525 can extend further over the orthosteric binding site and form additional van der Waals contacts with the proposed allosteric pocket (Supplemental Fig. 6). In addition, increasing the size of the fused ring at the 4- and 5-positions increases AE activity (Bruns et al., 1990). More recent studies showed that large substituents at the 4- and 5-positions also enhance AE activity (Romagnoli et al., 2008; Aurelio et al., 2009). These observations provide two possible explanations to account for differences in the AE activity of ATL525 and PD 81,723: the ability of ATL525 to form additional A_1R-AE interactions and an increased ability to trap agonists in the orthosteric binding pocket, thereby preventing exit from the receptor. Orthosteric agonist

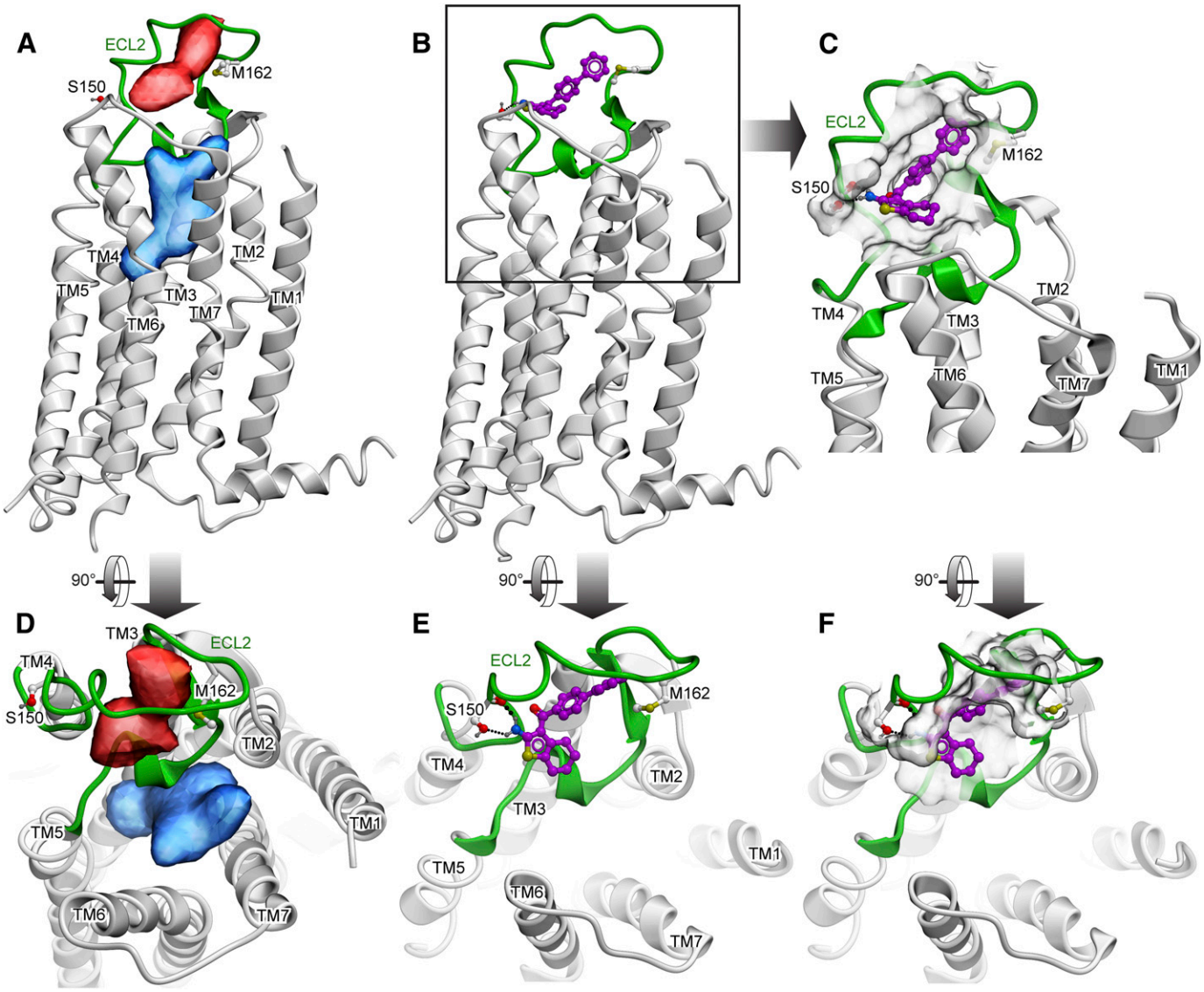

Fig. 4. ATL525 docked to the hA_1R homology model. (A) The hA_1R homology model (gray) based on the high-resolution crystal structure of $hA_{2A}R$ (PDB ID 3QAK). Residues S150 and M162, identified as being involved in AE signaling by site-directed mutagenesis in ECL2 (green), are shown as sticks. Ligand binding pockets were identified using ICM PocketFinder, including the orthosteric site (blue surface) and a pocket in ECL2 large enough to accommodate hA_1R AEs (red surface). (B) Allosteric enhancer, ATL525 (ball and stick), docked into the hA_1R ECL2 binding pocket of the ALiBERO-optimized hA_1R homology model (ribbon). (C) Enlarged view of ATL525 docked into the hA_1R homology model. (D, E, and F) Extracellular views of (A, B, and C), respectively, perpendicular to the plane of the membrane. AE atoms colored according to atom type; carbon, purple; sulfur, yellow; nitrogen, blue; oxygen, red. Dotted lines depict hydrogen bonds between ATL525 and S150.

trapping is likely bestowed by substitutions on the 4- and 5- positions of the thiophene ring.

Discussion

The binding modes of AEs are consistent with the established SAR (Bruns et al., 1990), in which the 2- and 3-positions of the thiophene are restricted to an amino group and a carbonyl-containing substituent, respectively, and various alkyl and aryl substituents are tolerated at the 4- and 5-positions (Supplemental Fig. 7). A key feature of 2-aminothiophenes is an intramolecular hydrogen bond between the 2-amino and the 3-keto groups, creating a ring coplanar with the thiophene ring (Bruns et al., 1990). The hydrogen bonding interaction to S150 may explain why acylation of the 2-amino group results in loss of AE activity (Bruns et al., 1990). The docked poses of the AEs in the potential AE binding site were consistent with the established SAR. The 2-amino group formed a hydrogen bond to S150, the 3-benzoyl group was directed toward the back of the pocket, and the 4- and 5-positions of the thiophene were solvent exposed (Fig. 4E). This docked conformation of ATL525 may explain the diversity of alkyl and aryl substituents that are tolerated in these positions (Bruns et al., 1990; Romagnoli et al., 2012).

We note that the hA_1R ECL2 site is similar to a computationally predicted ligand entry vestibule comprising ECL2 and ECL3 in the β_2-adrenergic receptor. Alprenolol, a nonselective β-adrenergic receptor antagonist, was predicted to pass through several metastable states in this vestibule as it enters the β_2-adrenergic receptor orthosteric site (Dror et al.,

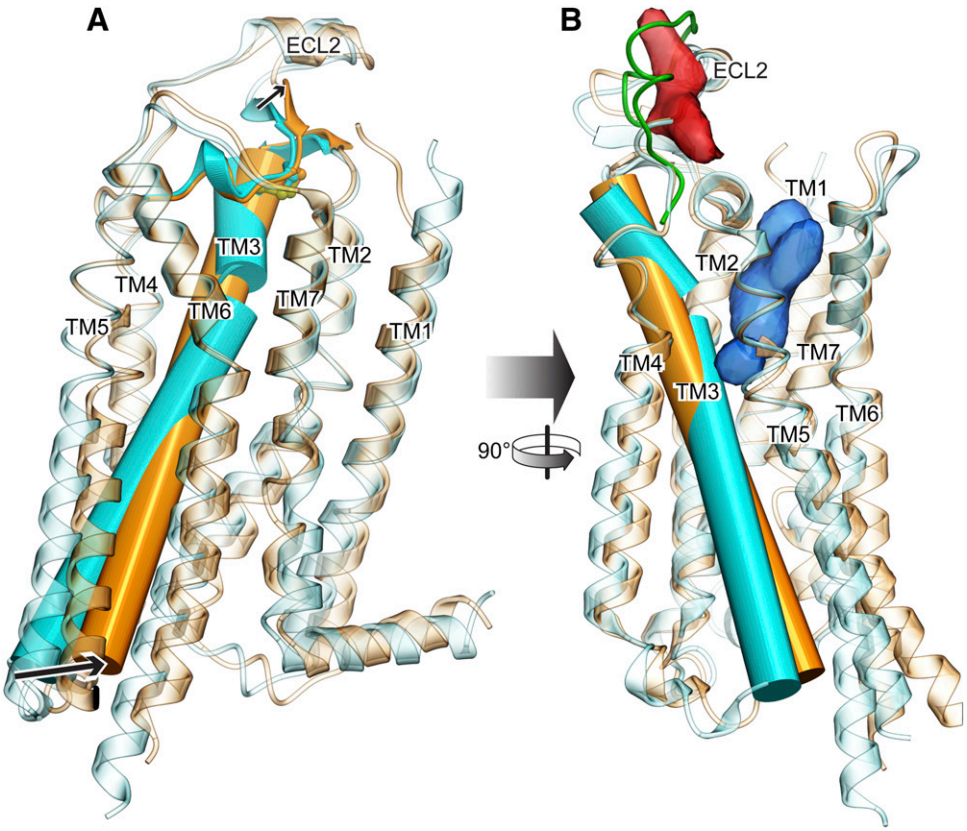

Fig. 5. Superimposed representative $A_{2A}R$ X-ray crystal structures (ribbons), with bound agonist (PDB ID 2YDV) (Lebon et al., 2011), TM3 (orange cylinders), and antagonist (PDB ID 4EIY) (Liu et al., 2012) (TM3 blue cylinders). Black arrows indicate movement of TM3 and ECL2 from the antagonist-bound state (blue) to the agonist-bound state (orange). (A and B) Two views showing the $A_{2A}R$ orthosteric site (blue surface), the model of ECL2 for hA_1R (green ribbon), and the proposed allosteric site (red surface) superimposed onto the $A_{2A}R$ crystal structures. Conserved disulfide bond shown as sticks.

2011). The proposed ECL2 AE pocket in A_1R may serve a similar function. The orthosteric agonist-bound receptor conformation may have a less accessible vestibule than the antagonist bound conformation, since agonists dissociate from A_1Rs much more slowly than antagonists with comparable equilibrium binding affinity (Casadó et al., 1993). On binding, AEs may sterically interfere with the exit of agonists and thereby slow ligand dissociation. This notion is supported by the observation that bulkier allosteric ligands, created by inserting larger cyclic linkers between the 4- and 5-positions on the thiophene ring, exhibit higher activity (Tranberg et al., 2002). In addition, this explanation is consistent with previous observations that AEs increase the B_{max} of orthosteric agonist ligands (Figler et al., 2003). Comparison of the agonist- and antagonist-bound crystal structures of $A_{2A}R$ (Fig. 5) demonstrates that agonist binding results in a conformational switch of TM3 and the antiparallel β-sheets in ECLs 1 and 2, and we suggest that this coupled movement facilitates AE binding to ECL2, locking the agonist in the orthosteric binding pocket until the AE dissociates.

The functional consequence of AE binding to active, receptor–G protein complexes is an apparent increase in the efficacy and duration of agonists. Site-directed mutagenesis and molecular modeling studies suggest that the AEs bind to a pocket in ECL2 that is flanked by S150 and M162 in the hA_1R. We propose that AEs function by occupying the identified ECL2 vestibule, thereby impeding agonist dissociation. Identification of the ECL2 vestibule provides an unprecedented opportunity to use pharmacological and structural data to guide the development of new AEs for hA_1R (Burford et al., 2011; Lane et al., 2013; Wang and Lewis, 2013).

Acknowledgments

The authors thank Dr. Manuel Rueda for assistance with ALiBERO and Dr. Irina Kufareva for useful discussions and for critically reading the manuscript. The authors thank Drs. Kevin Lynch and Ray Stevens for helpful discussions.

Authorship Contributions

Participated in research design: Kennedy, McRobb, R. Figler, Leonhardt, Purdy.

Conducted experiments: Kennedy, McRobb, Marshall.

Contributed new reagents or analytic tools: Kennedy, Leonhardt, H. Figler, Chordia.

Performed data analysis: Kennedy, McRobb, R. Figler, Linden, Abagyan, Yeager.

Wrote or contributed to the writing of the manuscript: Kennedy, McRobb, R. Figler, Linden, Abagyan, Yeager.

References

Abagyan R and Totrov M (1994) Biased probability Monte Carlo conformational searches and electrostatic calculations for peptides and proteins. *J Mol Biol* **235**: 983–1002.

Amoah-Apraku B, Xu J, Lu JY, Pelleg A, Bruns RF, and Belardinelli L (1993) Selective potentiation by an A_1 adenosine receptor enhancer of the negative dromotropic action of adenosine in the guinea pig heart. *J Pharmacol Exp Ther* **266**: 611–617.

An J, Totrov M, and Abagyan R (2005) Pocketome via comprehensive identification and classification of ligand binding envelopes. *Mol Cell Proteomics* **4**:752–761.

Aurelio L, Valant C, Flynn BL, Sexton PM, Christopoulos A, and Scammells PJ (2009) Allosteric modulators of the adenosine A_1 receptor: synthesis and pharmacological evaluation of 4-substituted 2-amino-3-benzoylthiophenes. *J Med Chem* **52**:4543–4547.

Baraldi PG, Zaid AN, Lampronti I, Fruttarolo F, Pavani MG, Tabrizi MA, Shryock JC, Leung E, and Romagnoli R (2000) Synthesis and biological effects of a new series of 2-amino-3-benzoylthiophenes as allosteric enhancers of A_1-adenosine receptor. *Bioorg Med Chem Lett* **10**:1953–1957.

Bhattacharya S, Youkey RL, Ghartey K, Leonard M, Linden J, and Tucker AL (2006) The allosteric enhancer PD81,723 increases chimaeric A_1/A_{2A} adenosine receptor coupling with G_s. *Biochem J* **396**:139–146.

Birdsall NJ and Lazareno S (2005) Allosterism at muscarinic receptors: ligands and mechanisms. *Mini Rev Med Chem* **5**:523–543.
Bruns RF and Fergus JH (1990) Allosteric enhancement of adenosine A_1 receptor binding and function by 2-amino-3-benzoylthiophenes. *Mol Pharmacol* **38**:939–949.
Bruns RF, Fergus JH, Coughenour LL, Courtland GG, Pugsley TA, Dodd JH, and Tinney FJ (1990) Structure-activity relationships for enhancement of adenosine A_1 receptor binding by 2-amino-3-benzoylthiophenes. *Mol Pharmacol* **38**:950–958.
Burford NT, Watson J, Bertekap R, and Alt A (2011) Strategies for the identification of allosteric modulators of G-protein-coupled receptors. *Biochem Pharmacol* **81**: 691–702.
Canals M, Lane JR, Wen A, Scammells PJ, Sexton PM, and Christopoulos A (2012) A Monod-Wyman-Changeux mechanism can explain G protein-coupled receptor (GPCR) allosteric modulation. *J Biol Chem* **287**:650–659.
Canals M, Sexton PM, and Christopoulos A (2011) Allostery in GPCRs: 'MWC' revisited. *Trends Biochem Sci* **36**:663–672.
Cardozo T, Totrov M, and Abagyan R (1995) Homology modeling by the ICM method. *Proteins* **23**:403–414.
Casadó V, Allende G, Mallol J, Franco R, Lluis C, and Canela EI (1993) Thermodynamic analysis of agonist and antagonist binding to membrane-bound and solubilized A_1 adenosine receptors. *J Pharmacol Exp Ther* **266**:1463–1474.
Chordia MD, Zigler M, Murphree LJ, Figler H, Macdonald TL, Olsson RA, and Linden J (2005) 6-aryl-8*H*-indeno[1,2-*d*]thiazol-2-ylamines: A_1 adenosine receptor agonist allosteric enhancers having improved potency. *J Med Chem* **48**: 5131–5139.
Christopoulos A and Kenakin T (2002) G protein-coupled receptor allosterism and complexing. *Pharmacol Rev* **54**:323–374.
Conn PJ, Christopoulos A, and Lindsley CW (2009) Allosteric modulators of GPCRs: a novel approach for the treatment of CNS disorders. *Nat Rev Drug Discov* **8**:41–54.
Daval J-L, von Lubitz DK, Deckert J, and Marangos PJ (1989a) Protective effects of cyclohexyladenosine following cerebral ischemia in the gerbil hippocampus. *Adv Exp Med Biol* **253B**:447–454.
Daval J-L, Von Lubitz DK, Deckert J, Redmond DJ, and Marangos PJ (1989b) Protective effect of cyclohexyladenosine on adenosine A_1-receptors, guanine nucleotide and forskolin binding sites following transient brain ischemia: a quantitative autoradiographic study. *Brain Res* **491**:212–226.
Dhalla AK, Chisholm JW, Reaven GM, and Belardinelli L (2009) A_1 adenosine receptor: Role in diabetes and obesity, in *Adenosine Receptors in Health and Disease* (Wilson CN and Mustafa SJ, eds) pp 271–295, Springer, Berlin Heidelberg.
Dror RO, Pan AC, Arlow DH, Borhani DW, Maragakis P, Shan Y, Xu H, and Shaw DE (2011) Pathway and mechanism of drug binding to G-protein-coupled receptors. *Proc Natl Acad Sci USA* **108**:13118–13123.
Ellis J, Seidenberg M, and Brann MR (1993) Use of chimeric muscarinic receptors to investigate epitopes involved in allosteric interactions. *Mol Pharmacol* **44**:583–588.
Figler H, Olsson RA, and Linden J (2003) Allosteric enhancers of A_1 adenosine receptors increase receptor-G protein coupling and counteract guanine nucleotide effects on agonist binding. *Mol Pharmacol* **64**:1557–1564.
Göblyös A and IJzerman AP (2011) Allosteric modulation of adenosine receptors. *Biochim Biophys Acta. Biomembranes* **1808**:1309–1318.
Heitman LH, Kleinau G, Brussee J, Krause G, and Ijzerman AP (2012) Determination of different putative allosteric binding pockets at the lutropin receptor by using diverse drug-like low molecular weight ligands. *Mol Cell Endocrinol* **351**:326–336.
Katritch V, Kufareva I, and Abagyan R (2011) Structure based prediction of subtype-selectivity for adenosine receptor antagonists. *Neuropharmacology* **60**:108–115.
Katritch V, Rueda M, and Abagyan R (2012) Ligand-guided receptor optimization, in Homology Modeling (Orry AJW and Abagyan R, eds) pp 189–205, Humana Press, New York.
Katritch V, Rueda M, Lam PC-H, Yeager M, and Abagyan R (2010) GPCR 3D homology models for ligand screening: lessons learned from blind predictions of adenosine A2a receptor complex. *Proteins* **78**:197–211.
Kollias-Baker C, Xu J, Pelleg A, and Belardinelli L (1994) Novel approach for enhancing atrioventricular nodal conduction delay mediated by endogenous adenosine. *Circ Res* **75**:972–980.
Kufareva I, Rueda M, Katritch V, Stevens RC, and Abagyan R; GPCR Dock 2010 participants (2011) Status of GPCR modeling and docking as reflected by community-wide GPCR Dock 2010 assessment. *Structure* **19**:1108–1126.
Lane JR, Abdul-Ridha A, and Canals M (2013) Regulation of G protein-coupled receptors by allosteric ligands. *ACS Chem Neurosci* **4**:527–534.
Lebon G, Warne T, Edwards PC, Bennett K, Langmead CJ, Leslie AGW, and Tate CG (2011) Agonist-bound adenosine A_{2A} receptor structures reveal common features of GPCR activation. *Nature* **474**:521–525.
Li X, Conklin D, Ma W, Zhu X, and Eisenach JC (2002) Spinal noradrenergic activation mediates allodynia reduction from an allosteric adenosine modulator in a rat model of neuropathic pain. *Pain* **97**:117–125.
Li X, Conklin D, Pan H-L, and Eisenach JC (2003) Allosteric adenosine receptor modulation reduces hypersensitivity following peripheral inflammation by a central mechanism. *J Pharmacol Exp Ther* **305**:950–955.
Lin H, Sassano MF, Roth BL, and Shoichet BK (2013) A pharmacological organization of G protein-coupled receptors. *Nat Methods* **10**:140–146.
Liu W, Chun E, Thompson AA, Chubukov P, Xu F, Katritch V, Han GW, Roth CB, Heitman LH, and IJzerman AP et al. (2012) Structural basis for allosteric regulation of GPCRs by sodium ions. *Science* **337**:232–236.
May LT, Leach K, Sexton PM, and Christopoulos A (2007) Allosteric modulation of G protein-coupled receptors. *Annu Rev Pharmacol Toxicol* **47**:1–51.
Mizumura T, Auchampach JA, Linden J, Bruns RF, and Gross GJ (1996) PD 81,723, an allosteric enhancer of the A_1 adenosine receptor, lowers the threshold for ischemic preconditioning in dogs. *Circ Res* **79**:415–423.
Narlawar R, Lane JR, Doddareddy M, Lin J, Brussee J, and Ijzerman AP (2010) Hybrid ortho/allosteric ligands for the adenosine A_1 receptor. *J Med Chem* **53**: 3028–3037.
Overington JP, Al-Lazikani B, and Hopkins AL (2006) How many drug targets are there? *Nat Rev Drug Discov* **5**:993–996.
Park SW, Kim JY, Ham A, Brown KM, Kim M, D'Agati VD, and Lee HT (2012) A1 adenosine receptor allosteric enhancer PD-81723 protects against renal ischemia-reperfusion injury. *Am J Physiol Renal Physiol* **303**:F721–F732.
Peeters MC, Wisse LE, Dinaj A, Vroling B, Vriend G, and Ijzerman AP (2012) The role of the second and third extracellular loops of the adenosine A1 receptor in activation and allosteric modulation. *Biochem Pharmacol* **84**:76–87.
Pietra D, Borghini A, Breschi MC, and Bianucci AM (2010) Enhancer and competitive allosteric modulation model for G-protein-coupled receptors. *J Theor Biol* **267**: 663–675.
Robeva AS, Woodard R, Luthin DR, Taylor HE, and Linden J (1996) Double tagging recombinant A_1- and A_{2A}-adenosine receptors with hexahistidine and the FLAG epitope: development of an efficient generic protein purification procedure. *Biochem Pharmacol* **51**:545–555.
Romagnoli R, Baraldi PG, Carrion MD, Cara CL, Cruz-Lopez O, Iaconinoto MA, Preti D, Shryock JC, Moorman AR, and Vincenzi F et al. (2008) Synthesis and biological evaluation of 2-amino-3-(4-chlorobenzoyl)-4-[*N*-(substituted) piperazin-1-yl]thiophenes as potent allosteric enhancers of the A_1 adenosine receptor. *J Med Chem* **51**: 5875–5879.
Romagnoli R, Baraldi PG, Carrion MD, Cara CL, Cruz-Lopez O, Salvador MK, Preti D, Tabrizi MA, Moorman AR, and Vincenzi F et al. (2012) Synthesis and biological evaluation of 2-amino-3-(4-chlorobenzoyl)-4-[(4-arylpiperazin-1-yl)methyl]-5-substituted-thiophenes: effect of the 5-modification on allosteric enhancer activity at the A_1 adenosine receptor. *J Med Chem* **55**:7719–7735.
Rueda M, Totrov M, and Abagyan R (2012) ALiBERO: evolving a team of complementary pocket conformations rather than a single leader. *J Chem Inf Model* **52**:2705–2714.
Stewart GD, Valant C, Dowell SJ, Mijaljica D, Devenish RJ, Scammells PJ, Sexton PM, and Christopoulos A (2009) Determination of adenosine A_1 receptor agonist and antagonist pharmacology using *Saccharomyces cerevisiae*: implications for ligand screening and functional selectivity. *J Pharmacol Exp Ther* **331**:277–286.
Tranberg CE, Zickgraf A, Giunta BN, Luetjens H, Figler H, Murphree LJ, Falke R, Fleischer H, Linden J, and Scammells PJ et al. (2002) 2-Amino-3-aroyl-4,5-alkylthiophenes: agonist allosteric enhancers at human $A(_1)$ adenosine receptors. *J Med Chem* **45**:382–389.
van der Klein PAM, Kourounakis AP, and IJzerman AP (1999) Allosteric modulation of the adenosine A_1 receptor: synthesis and biological evaluation of novel 2-amino-3-benzoylthiophenes as allosteric enhancers of agonist binding. *J Med Chem* **42**: 3629–3635.
Venkatakrishnan AJ, Deupi X, Lebon G, Tate CG, Schertler GF, and Babu MM (2013) Molecular signatures of G-protein-coupled receptors. *Nature* **494**: 185–194.
Voigtländer U, Jöhren K, Mohr M, Raasch A, Tränkle C, Buller S, Ellis J, Höltje H-D, and Mohr K (2003) Allosteric site on muscarinic acetylcholine receptors: identification of two amino acids in the muscarinic M_2 receptor that account entirely for the M_2/M_5 subtype selectivities of some structurally diverse allosteric ligands in *N*-methylscopolamine-occupied receptors. *Mol Pharmacol* **64**:21–31.
Wang C-IA and Lewis RJ (2013) Emerging opportunities for allosteric modulation of G-protein coupled receptors. *Biochem Pharmacol* **85**:153–162.
Wojcik M, Zieleniak A, and Wozniak LA (2010) New insight into A₁ adenosine receptors in diabetes treatment. *Curr Pharm Des* **16**:4237–4242.
Xu F, Wu H, Katritch V, Han GW, Jacobson KA, Gao Z-G, Cherezov V, and Stevens RC (2011) Structure of an agonist-bound human A_{2A} adenosine receptor. *Science* **332**:322–327.

Address correspondence to: Mark Yeager, Department of Molecular Physiology and Biological Physics, The University of Virginia School of Medicine, Sheridan G. Snyder Translational Research Building, 480 Ray C. Hunt Drive, Charlottesville, VA 22908. E-mail: yeager@virginia.edu; or Ruben Abagyan, Skaggs School of Pharmacy and Pharmaceutical Sciences, University of California, San Diego, 9500 Gilman Drive, La Jolla, CA 92093. E-mail: ruben@ucsd.edu